FULL PAPER

Copper(II) and Zinc(II) Complexes with a Photoactive Bridging Ligand Based on Carbazole: Synthesis, Structures, Electronic and Magnetic Properties

Eike T. Spielberg[a] and Winfried Plass*[a]

Dedicated to Professor Ekkehardt Fluck on the occasion of his 80th birthday

The synthesis of the new Schiff base ligand *N*-(4-methoxyphenyl)-3,4-bis(salicylidenimino)carbazole (H$_2$SalCarbOMe) is described. It readily reacts with copper(II) and zinc(II) ions to form metallacycles of the general formula [M$_2$(SalCarbOMe)$_2$] (M = Cu, Zn). Their structures are determined by X-ray crystallography and show significant differences for the coordination at the metal ion with a nearly tetrahedral arrangement for Zn^{II}, but a considerable distortion towards square-planar geometry for Cu^{II}. This in turn leads to substantial differences for the dihedral angles observed between the salicylidene and carbazole moieties. As a consequence different arrangements in the unit cell are observed, which becomes particularly obvious when the additional solvent molecules of crystallization are considered. For the Zn^{II} compound this leads to the incorporation of a chloroform and a methanol molecule in fixed positions, whereas in the structure of the Cu^{II} compound a higher number of solvent molecules (chloroform, methanol, and water) in highly disordered crystallographic positions is observed. The optical and magnetic properties have been characterized for both complexes. They both show two band fluorescence in the visible region with emission maxima at 531 and 586 nm for the Zn^{II} compound and 488 and 580 nm in the Cu^{II} complex. The electronic properties have been further elucidated by quantum chemical calculations. For the two copper(II) ions an antiferromagnetic interaction through the carbazole bridging ligand with an exchange coupling constant of $J = -3.1$ cm^{-1} is observed. ESR spectroscopy reveals a rhombic signal with g values [g_x, g_y, g_z] = [2.057, 2.125, 2.200] consistent with the distorted coordination geometry around the copper(II) ions.

Introduction

During recent years a lot of effort has been spent on the development of new magnetic materials.[1] The combination of magnetic characteristics with other properties, for example luminescence, promises new materials which may open up new fields of applications.[2] Metal compounds are ideal candidates for use as magnetic materials as metal ions with unpaired electrons are good carriers for magnetic moments because of their rather large momentum assembled in a *d*- or *f*-shell, the stability of the open shell compounds, and the possibility to tune their properties through the choice of the metal ion and the design of the coordination sphere.[3] In addition, optical properties can be tuned in a very distinct way in organic compounds.[4] The influence of several substituents on the absorbance and emission of chromophores is well established. A vast number of chromophores is known and most have been characterized extensively as far as the nature of transitions and their other optical properties are concerned. It is therefore desirable to combine magnetic ions with photoactive ligands.

Carbazoles are well known building blocks in organic photo- and electrochemistry.[5,6] *N*-aryl-substituted carbazoles constitute a subclass of triphenylamines, which have been extensively studied. The design of organic light-emitting diodes,[7] photovoltaic elements,[8] and other organic electronic devices[6,9] are only three fields of interest for this type of molecule. In addition, aryl-substituted carbazoles have been studied due to their unusual fluorescence behavior, which has been discussed in terms of twisted intramolecular charge transfer[10] and recently by other mechanisms.[11]

We report here the synthesis of an *N*-aryl-substituted carbazole bridging ligand containing two Schiff base-derived metal ion binding pockets. This ligand is utilized to generate a copper(II) complex combining magnetic interactions and the photophysical properties of carbazole derivatives. As zinc(II) ions are known to give very similar complexes in many cases, the corresponding zinc(II) complex has been synthesized as diamagnetic comparison, which excludes magnetic interactions.

[a] Institut für Anorganische und Analytische Chemie, Friedrich-Schiller-Universität Jena,
Humboldtstr. 8, 07743 Jena, Germany
Fax: +49-3641-948132
E-mail: sekr.plass@uni-jena.de

Results and Discussion

Synthesis and Complex Formation

The amine precursor 3,4-diamino-*N*-(4-methoxyphenyl)-carbazole (**1**) was synthesized by Ullmann-type coupling of carbazole with *p*-bromoanisole according a variation of the synthetic procedure described by Zhang et al.[12] and subsequent introduction of the amino groups by nitration and reduction with elemental hydrogen. The reaction of **1** with two equivalents of salicylaldehyde in methanol gives the Schiff base ligand H$_2$SalCarbOMe (**2**, Scheme 1).
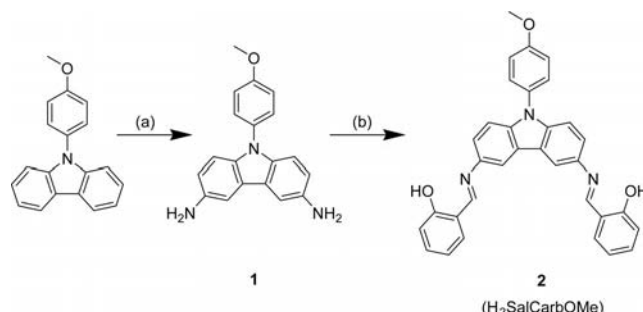
Scheme 1. Synthesis of **2**: (a) Cu(NO$_3$)$_2$, AcOH, Ac$_2$O; H$_2$, 55 bar, Raney nickel, AcOEt, 80 °C, 4 h. (b) Salicylaldehyde, MeOH, reflux, 10 min.

Ligand **2** reacts readily with copper(II) acetate and zinc(II) acetate in a solvent mixture of methanol/chloroform (1:1) to form the dinuclear complexes [Cu$_2$(SalCarbOMe)$_2$] (**3**) and [Zn$_2$(SalCarbOMe)$_2$] (**4**), respectively. Both complexes can be isolated as crystalline solids that contain cocrystallized solvent molecules. In **4** thermogravimetric and elemental analyses indicate the presence of one methanol and one chloroform molecule per dinuclear complex which are tightly bound. Whereas for **3** the solvent molecules were found to be only loosely bound leading to the decomposition of the crystals outside the mother liquor due to the loss of cocrystallized solvent molecules.

The formation of the complexes was further investigated by UV/Vis titrations of the ligand vs. copper and zinc acetate solutions. To a solution of **2** in methanol/chloroform (1:1) (copper: $c_{0,L} = 3.65 \times 10^{-5}$ M; zinc: $c_{0,L} = 3.08 \times 10^{-5}$ M) was added stepwise a solution of copper acetate ($c_{0,Cu} = 3.68 \times 10^{-3}$ M, 99 mL per step) or zinc acetate ($c_{0,Zn} = 3.68 \times 10^{-3}$ M, 85 mL per step). The spectra obtained are depicted in the Supporting Information (Figure S1). In both cases the two absorption bands of **2** at 358 and 380 nm (vide infra) decrease, while the bands of the corresponding metal complexes steadily increase giving rise to isosbestic points at 404 and 315 nm for copper acetate and 400 and 453 nm for zinc acetate. Their presence indicates a first order reaction. Hence there is direct formation of the dinuclear complexes without intermediates at a UV/Vis detectable concentration. The spectra were analyzed with *SpecReg* using nonlinear regression methods. Since a four component reaction is statistically improbable, the program only regards two compound reactions. Assuming a two-step mechanism for the formation of the metal com-

plexes (see Supporting Information) the equilibrium constants of these two reactions can be fitted to the experimental spectra giving the equilibrium constant K_{tot} for the total reaction; see Equation (1).
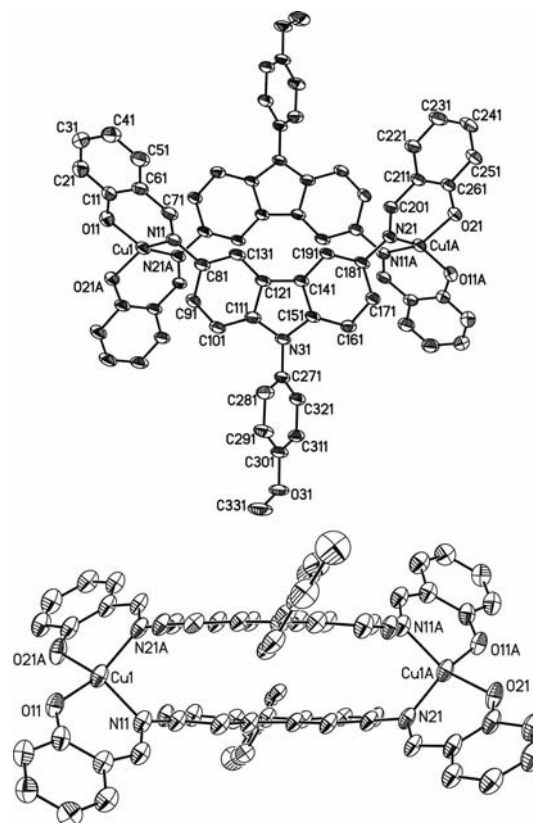
$$K_{tot} = K_I K_{II}^{1/2} \qquad (1)$$

For the titration with copper acetate the best fit was obtained with $K_I = 1.14 \times 10^7$ M^{-1} and $K_{II} = 9793$ M^{-1}, giving $K_{tot} = 1.13 \times 10^9$ M^{-1}. As only two species are detected in the spectra, K_I and K_{II} are strongly correlated. However, the value of K_{tot} remains constant within the expected tolerance (see Supporting Information). The large value of K_{tot} confirms the high overall stability of the dinuclear complex **3**.

Although the spectra for the formation of **4** look very similar (see Figure S1 in the Supporting Information) plausible results could not be obtained from the simulation of the spectroscopic data. This is most probably due to numerical problems within the fitting procedure.

Structural Characterization

The crystal structures of **3** and **4** were determined by X-ray crystallography. Both complexes crystallize in the space group P$\bar{1}$ with two independent centrosymmetric dinuclear molecules in the unit cell. As these two independent complex molecules show similar structural features for both

Figure 1. Molecular structure and numbering scheme for one of the independent complex units of **3**. Views perpendicular (top) and parallel (bottom) to the bridging carbazole. Hydrogen atoms are omitted for clarity, thermal ellipsoids are drawn at the 30% probability level.

compounds, only one is depicted for **3** and **4** in Figures 1 and 2, respectively. Selected bond lengths and angles for **3** and **4** are given in Tables 1 and 2, respectively.
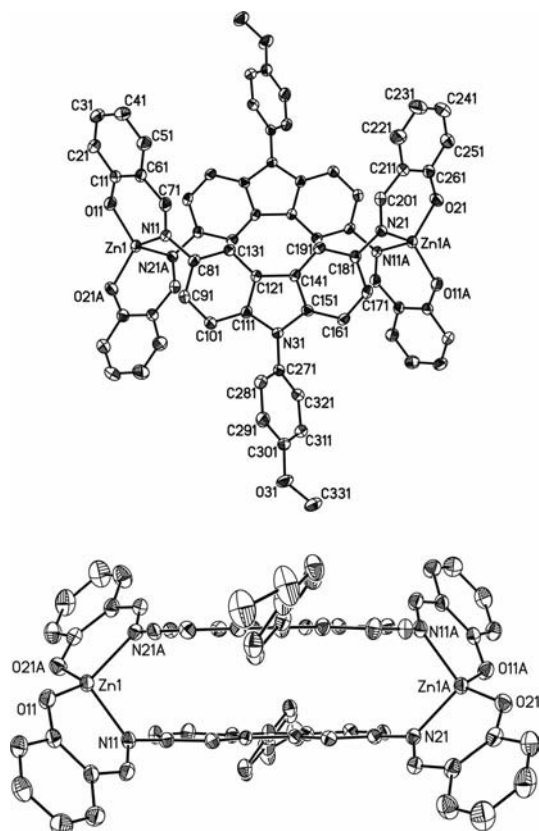

Figure 2. Molecular structure and numbering scheme for one of the independent complex units in **4**. Views perpendicular (top) and parallel (bottom) to the bridging carbazole. Hydrogen atoms are omitted for clarity, thermal ellipsoids are drawn at the 50% probability level.

Table 1. Selected bond lengths [pm] and angles [°] for **3**.

	$i = 1$	$i = 2$
Cui–O1i	188.2(4)	189.9(5)
Cui–O2iA	189.5(4)	189.9(4)
Cui–N1i	194.2(5)	195.0(6)
Cui–N2iA	193.9(5)	195.2(5)
O1i–Cui–O2iA	93.0(2)	97.3(2)
O1i–Cui–N1i	94.3(2)	94.0(2)
O1i–Cui–N2iA	148.2(2)	144.9(2)
O2iA–Cui–N1i	145.8(2)	142.6(2)
O2iA–Cui–N2iA	93.6(2)	94.4(2)
N1i–Cui–N2iA	97.5(2)	96.4(2)

In both **3** and **4** the metal ions are tetracoordinated by a [N$_2$O$_2$] donor set comprising the phenolate oxygen and imine nitrogen atoms of the salicylidene moiety of two bridging carbazole ligands. This leads to the formation of binuclear complex units [M$_2$(SalCarbOMe)$_2$] with coplanar carbazole moieties at distances of 313–322 pm. The resulting intramolecular metal–metal distances within the metallacycles, defined by the carbazole bridging ligand connected by two N–M–N moieties, are about 1070 pm (Cu1: 1072; Cu2: 1074; Zn1: 1067; Zn2: 1074 pm). The plane defined

Table 2. Selected bond lengths [pm] and angles [°] for **4**.

	$i = 1$	$i = 2$
Zni–O1i	190.6(2)	188.2(2)
Zni–O2iA	189.1(2)	189.9(2)
Zni–N1i	201.1(3)	201.6(2)
Zni–N2iA	200.4(2)	201.6(3)
O1i–Zni–O2iA	119.43(9)	122.44(10)
O1i–Zni–N1i	96.71(9)	97.59(10)
O1i–Zni–N2iA	122.72(9)	121.20(11)
O2iA–Zni–N1i	119.73(10)	120.50(10)
O2iA–Zni–N2iA	97.57(9)	97.03(10)
N1i–Zni–N2iA	100.75(9)	96.69(10)

by the two N–M–N moieties (Mi, N1i, N2iA, MiA, N1iA, N2i) of the metallacycle only slightly deviate from an orthogonal orientation with respect to the planes of the carbazole bridging ligands, leading to dihedral angles of 83 and 87° for **4** and 75 and 80° for **3**. Although the molecular structures of **3** and **4** are quite similar, this indicates some differences due to the nature of the coordinated metal ions, which might be attributed to their characteristic electronic structures. For a d^9 copper system a square planar arrangement should be favored, whereas for the d^{10} zinc system a tetrahedral coordination geometry can be expected. This is consistent with the bond angles observed at the metal centers of **3** and **4** (Tables 1 and 2).

Moreover, the characteristic differences in coordination geometry for the metal centers in **3** and **4** are also evident from the dihedral angles between the mean planes of the two coordinating salicylidene moieties, which in **3** deviate considerably from both ideal tetrahedral and square planar arrangements (Table 3). The related geometrical strain is also reflected in the large deviation of the copper ions from the respective mean planes.

Table 3. Dihedral angles [°] between mean planes defined by the salicylidene (Sal1i and Sal2i)[a] and the cabazole units (Carb$i$)[b] as well as for the tilting between the two benzene moieties (Ar1i and Ar2i)[c] within the carbazole units and the deviation d(Mi) [pm] for the metal centers from the salicylidene mean planes for the dinuclear complex units in **3** and **4**.

	M = Cu		M = Zn	
	$i = 1$	$i = 2$	$i = 1$	$i = 2$
∠Sal1i/Sal2i	47	50	78	74
d(Mi) form Sal1i	34	34	6	7
d(Mi) form Sal2i	59	51	13	17
∠Sal1i/Carb$i$	46	47	57	50
∠Sal2i/Carb$i$	38	28	46	42
∠Ar1i/Ar2i	6	6	2	1

[a] Salicylidene mean planes are defined by the following atoms. Sal1i: O1i, N1i, C1i, C2i, C3i, C4i, C5i, C6i, and C7i; Sal2i: O2i, N2i, C20i, C21i, C22i, C23i, C24i, C25i, and C26i. [b] Carbazole mean planes are defined by the following atoms. Carb$i$: C8i, C9i, C10i, C11i, C12i, C13i, C14i, C15i, C16i, C17i, C18i, and C19i. [c] Mean planes of the benzene rings of the Carbazoles are defined by the following atoms. Ar1i: C8i, C9i, C10i, C11i, C12i, and C13i; Ar2i: C14i, C15i, C16i, C17i, C18i, and C19i.

The shape of the coordination polyhedra of the metal centers in **3** and **4** can be analyzed utilizing continuous shape measures (CSM) introduced by Anvir et al.,[13] which

gives a quantitative measure for the distortion of a given coordination sphere from tetrahedral and square planar by the corresponding shape measures, S(T_d) and S(D_{4h}). These values give a measure for the difference from ideal geometry, where zero indicates ideal geometry. Data is given in Table 4. For **3** these values indicate a coordination geometry about halfway between tetrahedral and square planar, whereas for **4** a distorted tetrahedral geometry is observed.

Table 4. CSM parameters for the coordination geometries of **3** and **4** (for notation see text).

| | M = Cu | | M = Zn | |
	$i = 1$	$i = 2$	$i = 1$	$i = 2$
S$_i$(T_d)	10.34	8.71	1.70	1.86
S$_i$(D_{4h})	8.12	9.70	24.06	23.97
$\phi_i(T_d \rightarrow D_{4h})$[a]	53%	47%	20%	21%

[a] $\phi_i(T_d \rightarrow D_{4h})$ gives the angular fraction along the path from a tetrahedron to a square, for definition see ref.[15].

Significant differences between **3** and **4** are also found for the dihedral angles between the salicylidene and the carbazole moieties, with the somewhat larger angles observed in **4** (see Table 3). This is most probably related to the differences observed for the supramolecular structures of **3** and **4** (vide infra). In general, the overall structures of **3** and **4** are similar to those reported for the unsubstituted carbazole derivative.[14] Nevertheless, significant differences are observed for the supramolecular arrangement in the crystal structures, as the presence of the imine N–H group of the carbazole units leads to extensive hydrogen bonding, which is absent in **3** and **4**.

The crystal structures of **3** and **4** are primarily determined by π-π interactions between the aromatic moieties (salicylidene, carbazole, and methoxyphenyl substituents), leading to 2D-layered networks oriented along the crystallographic (100) plane (Figures S2 and S3, Supporting Information). The diameter of these sheets in **3** is found to be 1475 pm, whereas in **4** a somewhat smaller value of 1263 pm is observed. The two dinuclear complex units are found to have different orientations with respect to the 2D layers. The Cu1 and Zn1 units are arranged diagonally to the sheets with dihedral angles (metal–metal vector and normal vector) of 37 and 46°, respectively, whereas the Cu2 and Zn2 units are oriented almost coplanar within the layers with dihedral angles of 83 and 88°, respectively. The resulting angle between the metal–metal vectors of the two dinuclear units are 82 and 86° for **3** and **4**, respectively.

As a consequence the intermolecular metal–metal distances are considerably shorter than the intramolecular distances. Within the layers the shortest distances are found between the independent dinuclear units with values of 827 (Cu1 and Cu2) and 698 pm (Zn1 and Zn2). The shortest metal–metal distances across the layers are between dinuclear units containing Cu1 and Zn1 with values of 907 and 817 pm, respectively. This is consistent with the more dense packing in **4**.

Consequently, the major difference for the crystal structures arises from the amount and arrangement of incorporated solvent molecules. In compound **4** the methanol and

chloroform molecules are located near the phenolate oxygen atoms O11 and O22, respectively (Figure S4, Supporting Information). These crystallographic positions are fully occupied and no sign of disorder is observed, which is consistent with the solvent content in the isolated bulk material (vide supra). Data is given in Table 5. One dinuclear complex molecule is solely hydrogen-bonded to two methanol molecules, whereas the other is hydrogen-bonded to two chloroform molecules. Consequently, the crystal structure can be described as 2D layered networks of [Zn$_2$(SalCarbOMe)$_2$]·2CHCl$_3$ and [Zn$_2$(SalCarbOMe)$_2$]·2MeOH units with no solvent molecules located between the layers.

Table 5. Summary of bond lengths (pm) and angles (°) for the hydrogen bonding interactions in [Cu$_2$(SalCarbOMe)$_2$]·1.75CHCl$_3$·1.25MeOH·5.25H$_2$O (**3**)[a] and [Zn$_2$(SalCarbOMe)$_2$]·CHCl$_3$·MeOH (**4**).

D–H···A	d(D–H)	d(H···A)	∠D–H···A	d(D···A)
Compound **3** (see Figure S5, Supporting Information)				
C1C3–H···O21	100	216	172	316(2)
C1C4–H···O21	100	207	152	299(2)
C1C2–H···O12	100	246	144	332(2)
C1C2–H···O22	100	224	140	307(2)
Compound **4** (see Figure S4, Supporting Information)				
O1M–H···O11	84	197	157	276.2(4)
C2Cl–H···O22	100	211	152	302.8(5)

[a] Chloroform molecules in **3** are disordered with site occupation factors of 0.5 (C1C2, C1C3) and 0.25 (C1C4).

Although the dinuclear complex units [Cu$_2$(SalCarbOMe)$_2$] in compound **3** show a similar structural arrangement, significant differences are observed for the location of the solvent molecules. The chloroform molecules are disordered over four crystallographic positions, three of which enable hydrogen bonding to the phenolate oxygen atoms O12, O21, and O22 (Table 5 and Figure S5, Supporting Information). The remaining solvent molecules are located between the layers and disordered over several crystallographic positions. This leads to additional interactions with the methoxy-substituted phenyl rings of the bridging ligands of the dinuclear units containing Cu2, as they are oriented towards the surfaces of the layers. As a consequence this substituent at the carbazole unit is disordered over two positions.

Electronic Properties

Absorption spectra for **1** and **2** were recorded in THF solution, whereas those of **3** and **4** were measured in dichloromethane (Figure 3). The nature of the absorption bands was investigated utilizing semiempirical ZINDO/S calculations on DFT optimized structures. A comparison of simulated and measured spectra and a list of the character of orbitals near the HOMO–LUMO region are provided in Figure S6 and Table S1 of the Supporting Information. Fluorescence spectra were recorded by irradiating in the highest aromatic wavelength and are depicted in Figure 4. Excitation spectra were recorded to prove that all bands originate from the desired compounds.
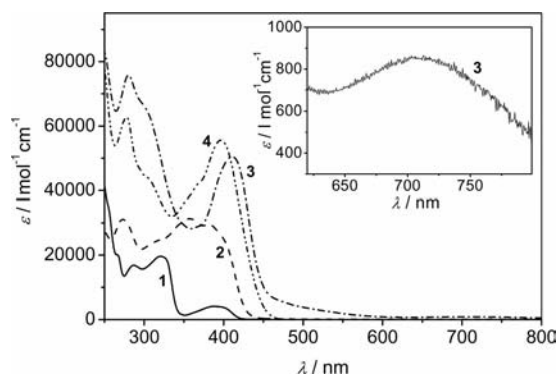
Figure 3. Absorption spectra of **1** in THF (solid line), **2** in THF (dashed line), **3** in CH$_2$Cl$_2$ (dash-dotted line), and **4** in CH$_2$Cl$_2$ (dash-dot-dotted line). The inset enlarges the absorption band of **3** at around 700 nm.
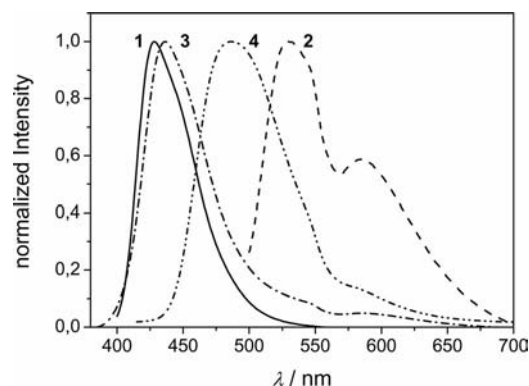

Figure 4. Fluorescence spectra of **1** (solid line), **2** (dashed line), **3** (dash-dotted line), and **4** (dash-dot-dotted line). The spectra were recorded in THF and have been normalized to one.

The spectrum of **1** consists mainly of four bands: the first with a maximum at around 390 nm (25640 cm^{-1}) with log ε = 3.61, the second around 320 nm (31250 cm^{-1}) with log ε = 4.29, the third at 287 nm (34840 cm^{-1}) with log ε = 4.23, and the fourth below 250 nm (> 40000 cm^{-1}) with log ε > 4.6. Fluorescence spectra of **1** recorded in THF show a strong band at around 428 nm (23360 cm^{-1}) with a shoulder at 446 nm (22420 cm^{-1}). The bands are shifted by 2280 and 3220 cm^{-1} compared to the absorption. The interpretation of the spectra is complicated by the obvious color dependence on the solvent used for recrystallization. Using ethanol results in a weakly colored solid, whereas using toluene gives better yields of a dark purple solid. However, the NMR spectra show no differences. The 320 nm transition is assigned as an n–π* transition from the lone pair of the central nitrogen atom into the aromatic backbone of the carbazole unit based on calculations.

Upon Schiff base condensation two new absorption bands at 271 nm (36900 cm^{-1}) with log ε = 4.66 and 358 nm (27930 cm^{-1}) with log ε = 4.61 arise, which can be attributed to transitions from the carbazole (backbone and nitrogen lone pair) into the π* of the Schiff base imine bond. The

fluorescence bands are shifted to 530 nm (18870 cm^{-1}) and 589 nm (16980 cm^{-1}) exhibiting Stokes shifts of 6770 and 8660 cm^{-1}, respectively. These large values indicate major reorganization after excitation. The intensity is strongly reduced compared to **1**, which is most probably due to new relaxation pathways along the salicylidene units.

Upon complexation the absorption band of the Schiff base ligand at 271 nm is only slightly shifted (**3**: 280 nm/35710 cm^{-1} with log ε = 4.87; **4**: 278 nm/35970 cm^{-1} with log ε = 4.80), whereas the band at 358 nm is shifted to a higher wavelength by about 40 nm [**3**: 412 nm (24270 cm^{-1}) with log ε = 4.70; **4**: 397 nm (25190 cm^{-1}) with log ε = 4.74]. The observed increase of the extinction coefficients can be explained by the fact that the complexes contain two ligand moieties per molecule.

Compound **3** shows two additional broad absorption bands of low intensity. The first is at around 480 nm (20830 cm^{-1}) with log ε = 3.71 and can be attributed to π*– π* transitions from the antibonding C–O bond orbital into antibonding orbitals at the C–N bond with contributions from the copper d orbitals. The second is at around 710 nm (14080 cm^{-1}) with log ε = 2.93 and can be attributed to π*– d(Cu) transitions from the antibonding C–O bond orbital into the copper d orbitals. Consequently, this absorption band is assigned as a phenolate to copper charge transfer transition.

In THF solution **3** shows a fluorescence band at 436 nm (22940 cm^{-1}) with a Stokes shift of 1330 cm^{-1}, whereas **4** shows a fluorescence maximum at 486 nm (20580 cm^{-1}) with a Stokes shift of 4610 cm^{-1}. In both cases additional weak fluorescence bands at around 530 and 590 nm are observed, which are reminiscent of **2**. This either indicates a partial dissociation in solution, which is unlikely based on the results of the UV/Vis titrations (vide supra), or a different fluorescent state, which is independent of metal coordination.

Square-wave voltammetry of **1** shows one oxidation process at 0.69 V (Figure S7, Supporting Information). Although this process is reversible, the differences between oxidation and reduction current suggests further decay reactions. Measurements of **2**, **3**, and **4** exhibited quite undefined oxidation processes at similar redox potentials. A possible explanation is the anodic polymerization described for carbazoles.[16]

Magnetic Properties

The temperature dependence of the magnetic susceptibility of **3** was determined in the temperature range between 2 and 300 K. Plots of $\chi_M = f(T)$ and $\chi_M T = f(T)$ are depicted in Figure 5. At high temperatures the value of $\chi_M T$ is 0.88 cm^3 K mol^{-1} that corresponds to the spin-only value for two independent copper(II) ions (0.75 cm^3 K mol^{-1} for g = 2). At very low temperatures $\chi_M T$ decreases indicating antiferromagnetic interactions between the copper centers. The $\chi_M T$ data were fitted utilizing the Bleaney–Blowers equation.[17]
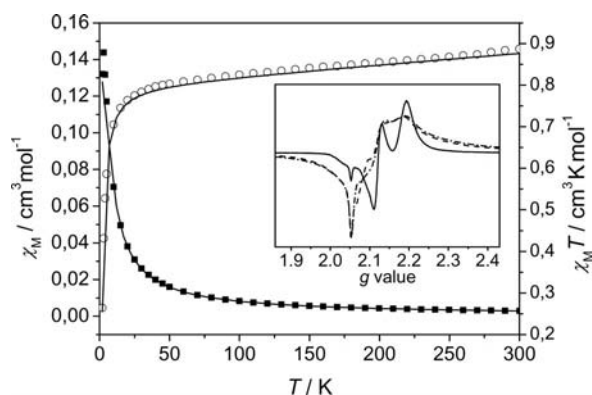
Figure 5. Temperature dependence of the magnetic susceptibility χ_M (black squares) and the product $\chi_M T$ (open circles) of **3** measured at an applied field of 2000 G. The solid lines represent the best simulation. Inset: ESR spectra of **3** recorded as a frozen solution at 77 K (solid line), a powdered sample at 77 K (dashed line), and at room temperature (dash-dotted line).

The best fit for Equation (2) is obtained with the parameters $g = 2.074(1)$, $J_{CuCu} = -3.14(1)$ cm^{-1}, and $\chi_{TIP} = 0.000268(4)$ cm^3 K mol^{-1} leading to an agreement factor R^2 of 0.99972. The observed antiferromagnetic coupling constant is in accordance with the value found for a similar system with an unsubstituted carbazole bridge.[14] A similar magnitude but ferromagnetic sign of the coupling constant is observed for *meta*-phenylene-bridged copper complexes, where spin-polarization effects are present.[18] However, a superexchange mechanism between the coupled copper centers and *meta*-phenylene bridges leads to antiferromagnetic interactions, but with significantly larger magnitude.[19]

$$\chi_M T = N\mu_B/(3k)[1 + 1/3\exp(-J_{CuCu}/(kT))]^{-1} + \chi_{TIP}T \qquad (2)$$

DFT calculations for the dinuclear copper complex utilizing the B3LYP functional have been performed to further investigate the magnetic properties. For these calculations the structural parameters of the Cu1 unit derived from the X-ray structure of **3** were used. The coupling constant is determined by the broken symmetry (BS) approach [$J = E(BS) - E(T)$, where $E(BS)$ and $E(T)$ are the energies of the broken symmetry and the triplet state, respectively].[20] These calculations yield a value of -3.5 cm^{-1}, which is in excellent agreement with the experimental coupling determined for **3**. Moreover, the alternating sign of the atomic spin populations derived by Mulliken population analysis indicates that a spin-polarization mechanism is in operation in the case of **3** (Figure S8, Supporting Information). The population analysis further shows that the delocalization of the spin densities at the copper centers into the carbazole bridging unit is quite small and comparable to that found for the delocalization into the salicylidene chelates. This is consistent with rather weak coupling between the copper centers through the bridging carbazole ligand. Moreover, it should be noted that spin density is not found at the carbazole nitrogen atom and consequently also no delocalization into the *p*-methoxyphenyl substituent is observed in the calculations.

ESR spectra for **3** were recorded on powder samples at room temperature and 77 K as well as on a frozen solution in chloroform at 77 K (see inset in Figure 5). The spectra can be simulated using the rhombic g values [g_x, g_y, g_z] = [2.057, 2.125, 2.200] leading to an isotropic value of $g_{iso} = 2.127$, which is in good agreement with the measured susceptibilities and DFT calculations on mononuclear model complexes (see Table 6). Moreover, the g values are consistent with the geometric distortion observed for the coordination environment of the copper centers in **3**, which is almost halfway between tetrahedral and square planar (cf. Table 4).[21] With increasing distortion, given by the rotation angle between the two chelate units, the normally observed axial ESR spectrum becomes rhombic. Rotation angles of around 50°, as observed in **3** ($\angle$Sal1i/Sal2i, see Table 3), lead to a clear separation of the two perpendicular components (g_y and g_x).[22]

Table 6. ESR parameters for **3** from simulation of experimental data and DFT calculations for mononuclear models of the copper centers of the two independent molecules (Cu1 and Cu2).

	g_x	g_y	g_z	g_{iso}
exp.	2.057	2.125	2.200	2.127
DFT Cu1	2.049	2.054	2.178	2.094
DFT Cu2	2.053	2.058	2.187	2.099

However, in the spectra two features are observed for the g_z component, a sharp signal and a very broad signal. This indicates the presence of two different entities, which is in agreement with the crystal structure of **3**, for which significant differences are observed for the hydrogen bonding interactions of the two crystallographic independent molecules (Cu1 and Cu2, vide supra). Both the sharp and the broad signal are also present in the spectrum of the frozen solution, with the sharp signal being less intense compared to the powder spectra. In line with the ESR spectra on the powdered samples it is therefore tempting to attribute this to the presence of an equilibrium of the complex [Cu$_2$(Sal-CarbOMe)$_2$] with its hydrogen bonded aggregates in solution, with the latter giving rise to the broad signal. As the large excess of solvent favors the hydrogen bonding, this causes the sharp signal to decrease, whereas the broad signal gains in intensity (Table 6).

Conclusions

We have described the synthesis of an *N*-(*p*-methoxyphenyl) substituted carbazole as a bridging ligand. This ligand contains two Schiff base-derived metal binding pockets and has been utilized for the synthesis of metallacyclic binuclear copper and zinc complexes [Cu$_2$(SalCarbOMe)$_2$] (**3**) and [Zn$_2$(SalCarbOMe)$_2$] (**4**). Both complexes show similar structural features, but significantly differ in the geometry of the metal coordination environment. For the zinc center slightly distorted tetrahedral geometry is observed, whereas the copper centers have a distorted coordination geometry halfway between tetrahedral and square planar. This leads to differences in the crystal packing with highly

disordered solvent molecules for **3**, which is also reflected in the ESR spectra. Magnetic measurements show a weak antiferromagnetic coupling between the two copper centers in **3**. The spectroscopic features show that most contributions to the observed low energy absorption bands arise from n–π* transitions with the lone pair of the carbazole nitrogen. However, for **3** significant contributions of the copper d orbitals are present leading to LMCT characteristic of these absorption bands. Further investigations will be focused on the interplay between photo activity and magnetism of the carbazole bridging system.

Experimental Section

Materials: The chemicals for synthesis were used as received without further purification. N-(p-Methoxyphenyl)carbazole was synthesized according to a literature procedure.[12] THF for fluorescence measurements was obtained from Roth as RotiSolv® ≥ 99.9% UV/IR grade and was used without further purification.

Instrumentation: ¹H, ¹³C, ¹H-¹H COSY, and ¹H-¹³C heteronuclear correlation NMR spectra were recorded with a Bruker Avance 400 MHz spectrometer. IR spectra were measured with a Bruker IFS55/Equinox spectrometer with a Raman unit FRA 106/S on samples prepared as KBr pellets. Mass spectra were measured with a Bruker MAT SSQ 710 spectrometer. Elemental analysis (C,H,N) were carried out with a Leco CHNS-932 and El Vario III elemental analyzers. Thermogravimetric analysis for powdered samples was performed with a NETZSCH STA409PC Luxx apparatus under constant flow of air ranging from room temperature up to 1000 °C with a heating rate of 1 °C/min. UV/Vis spectra were recorded with a VARIAN CARY 5000 UV/Vis spectrometer. Fluorescence spectra were recorded with a Jasco FP-6300 spectrofluorometer. ESR measurements were performed with a Bruker ESP 300E using X-Band (9 GHz). Magnetic susceptibilities were obtained from powdered samples in gelatin capsules using a Quantum-Design MPMSR-5S SQUID magnetometer equipped with a 5 T magnet in the range from 300 to 2 K (for details see ref.[23]). The measured data were corrected for diamagnetism of the capsules and the intrinsic diamagnetism of the sample, estimated by measurements on a similar ligand system.

3,4-Diamino-N-(4-methoxyphenyl)carbazole (1): $Cu(NO_3)_2 \cdot 3H_2O$ (7.94 g, 33 mmol) was added to a mixture of acetic acid (15 mL) and acetic acid anhydride (30 mL) and stirred for 10 min at room temperature. N-(4-Methoxyphenyl)carbazole (7.50 g, 27 mmol) was added slowly over five minutes. After adding acetic acid (15 mL) the resulting solution was stirred for an additional 30 min. The solution was poured into ice water (250 mL), the yellow precipitate was collected by filtration, and washed three times with water (150 mL). The product was dried for one day under reduced pressure at 70 °C. This solid was suspended in ethyl acetate and several spatulas of Raney nickel were added. Gaseous hydrogen was applied with a pressure of 55 bar. The mixture was stirred at 80 °C for 4 h. After cooling the nickel was removed by filtration and washed three times with ethyl acetate. After drying over Na_2SO_4 the solvent was removed to give the crude product (7.50 g). Recrystallization from toluene yielded 3,4-diamino-N-(p-methoxyphenyl)carbazole (5.54 g, 18.3 mmol, 67%); m.p. 320 °C (dec.). $C_{19}H_{17}N_3O$ (303.36): calcd. C 75.23, H 5.65, N 13.85; found C 75.15, H 5.73, N 13.94. Selected IR data (KBr): ṽ = 3377 [s, $\nu_{as}(NH_2)$], 3292 [s, $\nu_s(NH_2)$], 2956 (m), 2933 (m), 2838 [m, $\nu(OCH_3)$], 1613 [m, $\nu_{arom}(C–C)$], 1580 [m, $\nu_{arom}(C–C)$], 1514 [s, $\nu_{arom}(C–C)$], 1218 (s) cm⁻¹. ¹H NMR

(400 MHz, CDCl₃, 25 °C): δ = 3.84 (s, 3 H, OCH_3), 4.72 (s, 4 H, NH_2), 6.69–6.71 (m, 2 H, H^2), 7.00–7.02 (m, 2 H, H^3), 7.13–7.15 (m, 2 H, $H^{4,5}$), 7.15 (s, 2 H, H^1), 7.39–7.4 (m, 2 H, $H^{4,5}$) ppm. ¹³C NMR (100 MHz, CDCl₃, 25 °C): δ = 55.9, 104.3, 110.0, 115.3, 115.5, 123.6, 127.7, 131.5, 135.5, 142.1, 157.9 ppm. MS-EI: m/z (%) = 303 (100) [M], 288 (27) [M – CH₃], 31 (38) [OCH₃].

N-(4-Methoxyphenyl)-3,4-bis(salicylidenimino)carbazole (2): Salicylaldehyde (240 µL, 0.28 g, 2.3 mmol) was added to a suspension of 3,4-diamino-N-(4-methoxyphenyl)carbazole (0.35 g, 1.15 mmol) in methanol (20 mL). The suspension was heated for 10 min under reflux and allowed to cool to room temperature. The yellow precipitate was collected by filtration and washed with a small amount of methanol. After drying under reduced pressure product was obtained (0.48 mg, 0.94 mmol, 82%); m.p. 300 °C (dec.). $C_{33}H_{25}N_3O_3$ (511.58): calcd. C 77.48, H 4.93, N 8.21; found C 77.09, H 4.80, N 8.03. Selected IR data (KBr): ṽ = 3437 [s, $\nu(O–H)$], 3053 (w), 2930 (w), 2836 [w, $\nu(OCH_3)$], 1618 [s, $\nu(C=N)$], 1514 [s, $\nu_{arom}(C–C)$], 1285 (s), 1247 (s), 1149 (m), 1031 (m), 754 (s) cm⁻¹. ¹H NMR (400 MHz, CDCl₃, 25 °C): δ = 3.95 (s, 3 H, OCH_3), 6.8–7.6 (m, 16 H, H_{arom}), 8.11 (s, 2 H, H^7), 8.80 (s, 2 H, N=CH), 13.61 (s, 2 H, OH) ppm. ¹³C NMR (100 MHz, CDCl₃, 25 °C): δ = 55.7, 110.7, 112.5, 115.3, 117.2, 119.0, 119.6, 120.6, 123.7, 128.4, 129.7, 132.0, 132.7, 141.1, 141.4, 159.2, 160.5, 161.1 ppm. MS-ESI positive: m/z (%) = 512 (100) [M + H]⁺, 413 (28).

[Cu₂(SalCarbOMe)₂] (3): To a solution of **2** (102 mg, 0.2 mmol) in chloroform/methanol (1:1, 10 mL) was added $Cu(AcO)_2 \cdot H_2O$ (40 mg, 0.2 mmol) dissolved in chloroform/methanol (1:1, 2 mL). The resulting red solution was allowed to stand at room temperature for the solvent to slowly evaporate. Red brown crystals suitable for X-ray crystallography were obtained within a day. Total yield: 47 mg (0.04 mmol, 40%); m.p. 300 °C (dec.). $C_{66}H_{46}Cu_2N_6O_6 \cdot 0.8CHCl_3$ (1241.72): calcd. C 64.61, H 3.80, N 6.77; found C 64.68, H 3.81, N 6.78. Selected IR data (KBr): ṽ = 3435 [s, $\nu(O–H)$], 3052 [w, $\nu_{arom}(C–H)$], 2988 (w), 2927 (w), 1605 [vs, $\nu(C=N)$], 1530 (s), 1514 [vs, $\nu_{arom}(C–C)$], 1461 (s), 1444 (s), 1248 (s), 1148 (s), 757 (m) cm⁻¹. MS-ESI positive: m/z (%) = 1167 (100) [M + Na]⁺, 1146 (36), M⁺. ESR (X-band, powder, 77 K): g = [2.057, 2.125, 2.200].

[Zn₂(SalCarbOMe)₂] (4): To a solution of **2** (102 mg, 0.2 mmol) in chloroform/methanol (1:1, 10 mL) was added $ZnAc_2 \cdot 2H_2O$ (44 mg, 0.2 mmol) dissolved chloroform/methanol (1:1, 2 mL). The resulting orange-brown solution, which showed green fluorescence, was allowed to stand at room temperature for the solvent to slowly evaporate. Crystals suitable for X-ray crystallography were obtained within a day. Total yield: 52 mg (0.045 mmol, 45%); m.p. 400 °C (dec.). $C_{66}H_{46}N_6O_6Zn_2 \cdot CHCl_3 \cdot MeOH$ (1301.31): calcd. C 62.76, H 3.95, N 6.46; found C 62.50, H 3.63, N 6.45. Selected IR data (KBr): ṽ = 3435 [m, $\nu(O–H)$], 3044 (w), 3001 (w), 2957 (w), 2933 (w), 2905 (w), 2834 [w, $\nu(OCH_3)$], 1605 [vs, $\nu(C=N)$], 1534 (s), 1514 [vs, $\nu_{arom}(C–C)$], 1463 (s), 1442 (s), 1248 (s), 1173 (s), 1025 (m), 757 (m) cm⁻¹. MS-DEI: m/z (%) = 1151 (0.5) [L₂Zn₂]⁺, 575 (0.1) [LZn]⁺, 83 (100), 47 (21).

Computational Details: The evaluation of the absorption spectra is based on structures which were optimized with DFT calculations utilizing the BP86 functional[24] with the RI approximation and def2-TZVP basis sets[25–27] as provided by the program package TurboMole.[28] Absorption spectra were calculated for the optimized structures using the ZINDO/S method[29] as implemented within the ORCA program package[30,31] and plotted with the *orca_mapspc* functionality. To study the magnetic properties of **3** DFT calculations with the program package ORCA[30] were performed utilizing the hybrid functional B3LYP[32] in combination with def2-

SVP (C,N,O,H) and def2-TZVP (Cu) basis sets.[25,26] The geometry was taken from the crystallographic structure for the dinuclear unit Cu1, with the positions of the hydrogen atoms optimized. The data was analyzed according the phenomenological Heisenberg Hamiltonian H = $-JS_1S_2$, where the coupling constant J is given by the energy difference between the relevant triplet and singlet states [J = E(S) – E(T)]. Therefore, a negative value of J indicates antiferromagnetic coupling with a triplet ground state. The BS approach originally proposed by Noodleman was used to cope with the DFT inherent problem that the singlet state cannot be expressed by a single determinant.[33] In this formalism, the energy of the singlet state is computed on the basis of a single determinate of broken spin and space symmetry built up by localizing spin up and spin down electrons onto the two copper centers, which is not a spin eigenstate. Although the original formalism was based on spin projection to extract the singlet energy, it has been shown that this energy can be directly estimated from the energy of the BS solution [E(BS)] without performing any spin projection according to J = E(BS) – E(T). This procedure is in accordance with the proposal of Perdew et al., who suggested that the BS determinant is the correct solution of the Kohn–Sham equations for the singlet state.[34] The ESR parameters were calculated with the program package ORCA[30,35] utilizing the one parameter hybrid functional PBE0[36] in combination with VDZ (C,N,O,H) and CoreProp (Cu) basis sets.[25,37] The calculations were performed on mononuclear model systems for the two crystallographic independent molecules (Cu1 and Cu2), derived from the crystal structure of **3**, that contain the full coordination environment of the copper ions, with the carbazole moiety replaced by a phenyl group and the positions of the hydrogen atoms optimized.

Electrochemical Measurements: Cyclic square-wave voltammetric measurements were carried out by a three-electrode technique using a home-built computer-controlled instrument. The experiments were performed in acetonitrile solutions containing 0.25 M tetra-*n*-butylammonium hexafluorophosphate under a blanket of solvent saturated with argon. Ag/AgCl was used as the reference electrode in acetonitrile containing 0.25 M tetra-*n*-butylammonium chloride. The working electrode was a hanging mercury drop. The potentials reported in this paper refer to the ferrocenium/ferrocene couple, which has been measured at the end of each experiment (for details see ref.[38]).

X-ray Crystallography: The crystallographic data were collected with a Nonius KappaCCD diffractometer using graphite-monochromated Mo-K_α radiation (71.073 pm). A summary of crystallographic and structure refinement data is given in Table 7. The structure was solved by direct methods with SHELXS-97 and was full-matrix least-squares refined against F^2 using SHELXL-97.[39] All non-hydrogen atoms were refined anisotropically. Hydrogen atoms were calculated and treated as riding atoms with fixed thermal parameters. For the dinuclear unit containing Cu2 of compound **3** the *p*-methoxyphenyl substituent on the carbazole was found to be disordered over two positions in a 3:1 ratio. The chloroform molecules are disordered over four positions with occupancy factors of 0.5 (C1C1, C1C2, and C1C3) and 0.25 (C1C4), whereas the methanol molecules are disordered over three positions with occupancy factors of 0.5 (C1M1 and C1M2) and 0.25 (C1M3). The water molecules in the crystal structure are disordered over 16 positions and hydrogen bonded to the methanol molecules and the chloroform molecule with C1C1, which is not hydrogen bonded to one of the independent dinuclear copper complexes (Cu1 and Cu2). The latter molecules are all located in the region between the 2D layers observed for **3** (Figure S2, Supporting Information).

Table 7. Summary of crystallographic data for [Cu$_2$(SalCarbOMe)$_2$]·1.75CHCl$_3$·1.25MeOH·5.25H$_2$O (**3**) and [Zn$_2$(SalCarbOMe)$_2$]·CHCl$_3$·MeOH (**4**).

	3	4
Formula	C$_{69}$H$_{63.25}$Cl$_{5.25}$Cu$_2$N$_6$O$_{12.5}$	C$_{68}$H$_{51}$Cl$_3$N$_6$O$_7$Zn$_2$
Formula weight	1489.70	1301.24
Crystal system	triclinic	triclinic
Space group	$P\bar{1}$	$P\bar{1}$
a [pm]	15.6401(9)	14.3107(3)
b [pm]	15.9390(8)	14.9621(6)
c [pm]	16.8759(9)	16.9319(5)
α [°]	63.449(3)	112.754(1)
β [°]	71.314(2)	96.694(2)
γ [°]	77.162(2)	112.014(2)
V [10^6 pm^3]	3549.4(3)	2950.92(16)
Z	2	2
T [K]	183(2)	183(2)
d_{calc} [g cm^{-3}]	1.394	1.464
$F(000)$	1533	1336
μ [mm^{-1}]	0.861	1.011
θ range [°]	1.70–27.47	2.36–27.47
Measured data	24816	21441
Unique data (R_{int})	16007 (0.0505)	13406 (0.0369)
Data [$I > 2\sigma(I)$]	8401	9104
GOF on F^2	1.028	1.018
R_1 (observed data)	0.0853	0.0491
wR_2 (all data)	0.2637	0.1127

CCDC-774835 (for **3**) and -774836 (for **4**) contain the supplementary crystallographic data for this paper. These data can be obtained free of charge from The Cambridge Crystallographic Centre via www.ccdc.cam.ac.uk/data-request/cif.

Supporting Information (see footnote on the first page of this article): UV/Vis titrations with ligand **2** and copper and zinc salts, graphics showing the crystal packing and hydrogen bonding for **3** and **4**, comparison of measured and computed absorption spectra for compounds **1**–**4**, square-wave voltammograms of compound **1**, Mulliken spin population for the broken symmetry state derived from DFT calculations on **3**, and details on the orbital character in the HOMO–LUMO region derived from ZINDO/S calculations on **3**.

Acknowledgments

[1] a) J. S. Miller, M. Drillon (Eds.), *Magnetism: Molecules to Materials*, vol. I–V, Wiley-VCH, Weinheim, Germany, **2001**–**2005**; b) O. Kahn, *Acc. Chem. Res.* **2000**, *33*, 647–657; c) D. Gatteschi, R. Sessoli, J. Villain, *Molecular Nanomagnets*, Oxford University Press, Oxford, **2006**; d) W. Plass, *Chem. Unserer Zeit* **1998**, *32*, 323–333; e) A. Cornia, A. F. Costantino, L. Zobbi, A. Caneschi, D. Gatteschi, M. Mannini, R. Sessoli, *Struct. Bonding (Berlin)* **2006**, *122*, 133–161.

[2] a) Y. Zheng, F. Cardinali, N. Armaroli, G. Accorsi, *Eur. J. Inorg. Chem.* **2008**, *12*, 2075–2080; b) M.-J. Li, Z. Chen, V. W.-W. Yam, Y. Zu, *ACS Nano* **2008**, *2*, 905–912; c) Y. Zhang, S. Pan, X. Teng, Y. Luo, G. Li, *J. Phys. Chem. C* **2008**, *112*, 9623–9626; d) R.-S. Zhou, L. Ye, H. Ding, J.-F. Song, X.-Y. Xu, J.-

Q. Xu, *J. Solid State Chem.* **2008**, *18*, 567–575; e) L.-Q. Yu, R.-D. Huang, Y.-Q. Xu, T.-F. Liu, W. Chu, C.-W. Hu, *Inorg. Chim. Acta* **2008**, *361*, 2115–2122; f) C. A. Black, J. S. Costa, W. T. Fu, C. Massera, O. Roubeau, S. J. Teat, G. Aromi, P. Gamez, J. Reedijk, *Inorg. Chem.* **2009**, *48*, 1062–1068.

[3] W. Plass, *Coord. Chem. Rev.* **2009**, *253*, 2286–2295.

[4] S. R. Marder, B. Kippelen, A. K.-Y. Jen, N. Peyghambarian, *Nature* **1997**, *388*, 845–851.

[5] a) J. Morin, M. Leclerc, D. Ades, A. Siove, *Macromol. Rapid Commun.* **2005**, *26*, 761–778; b) S. Grigalevicius, *Synth. Met.* **2006**, *156*, 1–12.

[6] O. Paliulis, J. Ostrauskaite, V. Gaidelis, V. Jankauskas, P. Strohriegl, *Macromol. Chem. Phys.* **2003**, *204*, 1706–1712.

[7] a) W.-Y. Wong, C.-L. Ho, Z.-Q. Gao, B.-X. Mi, C.-H. Chen, K.-W. Cheah, Z. Lin, *Angew. Chem. Int. Ed.* **2006**, *45*, 7800–7803; b) W.-Y. Wong, L. Liu, D. Cui, L. M. Leung, C.-F. Kwong, T.-H. Lee, H.-F. Ng, *Macromolecules* **2005**, *38*, 4970–4976; c) D. Velasco, S. Castellanos, M. Lopez, F. Lopez-Calahorra, E. Brillas, L. Julia, *J. Org. Chem.* **2007**, *72*, 7523–7532.

[8] T. Xu, R. Lu, X. Liu, X. Zheng, X. Qiu, Y. Zhao, *Org. Lett.* **2007**, *9*, 797–800.

[9] Y. Song, C. Di, Z. Wei, T. Zhao, W. Xu, Y. Liu, D. Zhang, D. Zhu, *Chem. Eur. J.* **2008**, *14*, 4731–4740.

[10] a) W. Rettig, M. Zander, *Chem. Phys. Lett.* **1982**, *87*, 229–234; b) F. Evers, J. Giraud-Girard, S. Grimme, J. Manz, C. Monte, M. Oppel, W. Rettig, P. Saalfrank, P. Zimmermann, *J. Phys. Chem. A* **2001**, *105*, 291–2924; c) S. Kapelle, W. Rettig, R. Lapouyade, *Chem. Phys. Lett.* **2001**, *348*, 416–424; d) T. Xu, R. Lu, X. Liu, P. Chen, X. Qiu, Y. Zhao, *J. Org. Chem.* **2008**, *73*, 1809–1817.

[11] A. Samanta, S. Saha, R. W. Fessenden, *J. Phys. Chem. A* **2001**, *105*, 5438–5441.

[12] H. Zhang, Q. Cai, D. Ma, *J. Org. Chem.* **2005**, *70*, 5164–5173.

[13] S. Keinan, D. Avnir, *Inorg. Chem.* **2001**, *40*, 318–323.

[14] A. R. Paital, A.-Q. Wu, Guo, G. Aromi, J. Ribas-Arino, D. Ray, *Inorg. Chem.* **2007**, *46*, 2947–2949.

[15] J. Cirera, E. Ruiz, S. Alvarez, *Chem. Eur. J.* **2006**, *12*, 3162–3167.

[16] J. Ambrose, R. Nelson, *J. Electrochem. Soc.* **1968**, *115*, 1159–1164.

[17] O. Kahn, *Molecular Magnetism*, Wiley-VCH, Weinheim **1993**.

[18] a) T. Glaser, H. Theil, M. Heidemeier, *C. R. Chim.* **2008**, *11*, 1121–1136; b) E. T. Spielberg, W. Plass, *Eur. J. Inorg. Chem.* **2010**, 3093–3096.

[19] a) D. Plaul, A. Buchholz, H. Görls, W. Plass, *Polyhedron* **2007**, *26*, 4581–4590; b) D. Plaul, D. Geibig, H. Görls, W. Plass, *Polyhedron* **2009**, *28*, 1982–1990.

[20] a) W. Plass, A. Pohlmann, J. Rautengarten, *Angew. Chem. Int. Ed.* **2001**, *40*, 4207–4210; b) W. Plass, *Angew. Chem. Int. Ed. Engl.* **1996**, *35*, 627–631; c) E. T. Spielberg, M. Fittipaldi, D. Geibig, D. Gatteschi, W. Plass, *Inorg. Chim. Acta* **2010**, *363*, 4269–4276.

[21] S. Keinan, D. Avnir, *J. Chem. Soc., Dalton Trans.* **2001**, 941–947.

[22] a) S. K. Hoffmann, J. Goslar, *J. Solid State Chem.* **1982**, *44*, 343–353; b) A. Bonamartini-Corradi, L. P. Battaglia, J. Rubenaker, R. D. Willett, T. E. Grigereit, P. Zhou, J. E. Drumheller, *Inorg. Chem.* **1993**, *32*, 3859–3863.

[23] a) W. Plass, *Angew. Chem. Int. Ed. Engl.* **1996**, *35*, 627–631; b) W. Plass, *Inorg. Chem.* **1997**, *36*, 2200–2205.

[24] a) J. P. Perdew, *Phys. Rev. B* **1986**, *33*, 8822–8824; b) A. D. Becke, *Phys. Rev. A* **1988**, *38*, 3098–3100.

[25] A. Schäfer, H. Horn, R. Ahlrichs, *J. Chem. Phys.* **1992**, *97*, 2571–2577.

[26] F. Weigend, R. Ahlrichs, *Phys. Chem. Chem. Phys.* **2005**, *7*, 3297–3305.

[27] F. Weigend, *Phys. Chem. Chem. Phys.* **2006**, *8*, 1057–1065.

[28] a) R. Ahlrichs, M. Bär, M. Häser, H. Horn, C. Kölmel, *Chem. Phys. Lett.* **1989**, *162*, 165–169; b) O. Treutler, R. Ahlrichs, *J. Chem. Phys.* **1995**, *102*, 346–354; c) M. von Arnim, R. Ahlrichs, *J. Comput. Chem.* **1998**, *19*, 1746–1757; d) M. von Arnim, R. Ahlrichs, *J. Chem. Phys.* **1999**, *111*, 9183–9190; e) R. Ahlrichs, *Phys. Chem. Chem. Phys.* **2004**, *6*, 5119–5121.

[29] a) J. Ridley, M. C. Zerner, *Theor. Chim. Acta* **1973**, *32*, 111–134; b) A. D. Bacon, M. C. Zerner, *Theor. Chim. Acta* **1979**, *53*, 21–54; c) M. C. Zerner, G. H. Loew, R. F. Kirchner, U. T. Mueller-Westerhoff, *J. Am. Chem. Soc.* **1980**, *102*, 589–599; d) W. P. Anderson, W. D. Edwards, M. C. Zerner, *Inorg. Chem.* **1986**, *25*, 2728–2732.

[30] F. Neese, *ORCA*, ab initio density-functional and semiempirical program package, version 2.7, University of Bonn, Germany, **2008**.

[31] T. Petrenko, F. Neese, *J. Chem. Phys.* **2007**, *127*, 1664319.

[32] a) A. D. Becke, *J. Chem. Phys.* **1993**, *98*, 5648–5652; b) C. Lee, W. Yang, R. G. Parr, *Phys. Rev. B* **1988**, *37*, 785–789.

[33] L. Noodleman, *J. Chem. Phys.* **1981**, *74*, 5737–5743.

[34] a) J. P. Perdew, A. Savin, K. Burke, *Phys. Rev. A* **1995**, *51*, 4531–4541; b) J. P. Perdew, M. Ernzerhof, K. Burke, A. Savin, *Int. J. Quantum Chem.* **1997**, *61*, 197–205.

[35] F. Neese, *J. Chem. Phys.* **2001**, *115*, 11080–11096.

[36] C. Adamo, V. Barone, *J. Chem. Phys.* **1999**, *110*, 6158–6170.

[37] a) K. Eichkorn, O. Treutler, H. Öhm, M. Häser, R. Ahlrichs, *Chem. Phys. Lett.* **1995**, *240*, 283–289; b) K. Eichkorn, F. Weigend, O. Treutler, R. Ahlrichs, *Theor. Chem. Acc.* **1997**, *97*, 119–124; c) A. J. H. Wachters, *J. Chem. Phys.* **1970**, *52*, 1033–1036; d) *TurboMole basis sets:* ftp://ftp.chemie.uni-karlsruhe.de/pub/basen and ftp://ftp.chemie.uni-karlsruhe.de/pub/jbasen; e) R. Ahlrichs and co-workers, unpublished results.

[38] a) S. Nica, A. M. Rudolph, H. Görls, W. Plass, *Inorg. Chim. Acta* **2007**, *360*, 1743–1752; b) S. Nica, A. Buchholz, M. Rudolph, A. Schweizer, M. Wächtler, H. Breitzke, G. Buntkowsky, W. Plass, *Eur. J. Inorg. Chem.* **2008**, 2350–2359.

[39] G. Sheldrick, *SHELXS-97* and *SHELXL-97*, University of Göttingen, Germany, **1997**.